

Investigating Pulses in Cables

Yunran Yang
Jacqueline Zhu

1 Abstract

This lab investigated the propagation of electrical pulses first in transmission lines and second in coaxial cables to analyze the effects of signal delay and pulse attenuation. In **Exercise 1**, electric pulses propagated down a 41 LC unit transmission line with an experimental propagation speed of $0.273 \times 10^6 \pm 0.0019$ LC-units/s, and a theoretical value of 0.258×10^6 LC-units/s. In **Exercise 2**, electric pulses propagated through a 15.09 m polyethylene-dielectric coaxial cable. The experimental speeds for open, short, and 100Ω terminations in the 15.09 m cable were $1.95 \times 10^8 \pm 6.6 \times 10^6$ m/s, $1.92 \times 10^8 \pm 2.00 \times 10^7$ m/s, and $1.96 \times 10^8 \pm 6.54 \times 10^7$ m/s, respectively. Lastly, the highest attenuation factor was found for the open circuit, -1.34 ± 0.012 dB/m, while the lowest occurred in the short circuit, -0.1440 ± 0.00081 dB/m.

2 Introduction

In AC and DC circuit theory, signal propagation is assumed to be instantaneous, allowing circuits to react immediately to changes. In reality, signals propagate at a finite speed, determined by the physical properties of the transmission medium. Transmission lines, such as coaxial cables, are essential for transmitting electrical signals in telecommunications, signal processing, and energy distribution. These cables consist of inductors (L_0) and capacitors (C_0) per unit length, which govern signal propagation. This lab aims to analyze the realistic behavior of electric pulses in transmission lines and coaxial cables.

Measuring propagation speed is crucial for ensuring efficient energy transfer, minimizing signal distortion, and optimizing system performance in applications relying on precise signal timing. The speed of signal propagation is determined by L_0 and C_0 and is given by:

$$v = \frac{1}{\sqrt{L_0 C_0}} \quad (1)$$

For coaxial cables, the propagation speed can also be expressed as

$$v = \frac{1}{\sqrt{\mu\epsilon}} \quad (2)$$

where $\mu = 1$ is the magnetic permeability of the dielectric, and $\epsilon = 2.25$ is the permittivity of the dielectric for this experiment.

The characteristic impedance Z_0 is defined as the ratio of voltage to current in a traveling wave and represents the load impedance required at the cable's termination to prevent reflections. When the load impedance deviates from Z_0 , reflections occur, leading to energy loss and signal degradation. Z_0 is given by:

$$Z_0 = \sqrt{\frac{L_0}{C_0}} \quad (3)$$

Signal attenuation is another critical consideration in transmission line analysis. It quantifies the energy lost as the signal propagates and can be measured as:

$$attenuation = 10 \log_{10} \left(\frac{V_{\text{reflected}}}{V_{\text{initial}}} \right)^2 \quad (4)$$

3 Methods

3.1 Materials

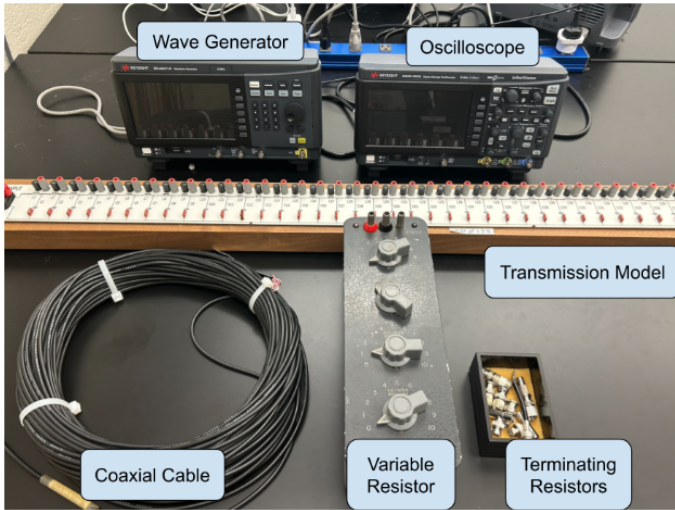


Figure 1: Photo of the experimental materials

The following materials are required for this lab:

- 41 LC unit transmission model
- Digital oscilloscope (Keysight DSOX1202G)
- Wave generator (Keysight EDU33211A)
- 15.09 m coaxial cable
- Variable resistor (Decade Resistor Type 1432-J)
- Terminating resistors with various resistances
- Connecting TEE pieces and cables

3.2 Methods

3.2.1 Exercise 1: Transmission Line

In Exercise 1, a 41 LC unit transmission line and waveform generator were used to measure the delay time between the transmitted and reflected pulses. The procedure was as follows:

1. One end of the TEE connector was connected to the waveform generator, and the other end was connected to Channel 1 of the oscilloscope.

The end of the transmission line was connected to Channel 2 through a second TEE connector (Figure 4 in Appendix 6.2).

2. The pulse width was manually set to $75 \mu\text{s}$ and the frequency to 300 Hz. The pulse width and frequency were varied until a returned pulse was observed on the oscilloscope.
3. Channel 1 (yellow) measured the input waveform, while Channel 2 (green) measured the output wave (Figure 5 in 6.2). The difference between these waves corresponds to the delay time.
4. Variable resistor was connected to the end of the transmission line. The resistance was adjusted until no reflected pulse was observed, giving impedance matching of 342Ω to the LC model resistance of 400Ω .
5. The delay time of the transmitted and reflected pulses was measured by moving the wire on the transmission line by two LC units at a time. For each LC unit, the delay time was recorded 3 times to get the average delay time. Measuring every two LC units gave us enough time to conduct 3 trials for each measurement; we prioritized quality of each data point over quantity.
6. The delay time was measured as the difference between the rising edges of the transmitted and reflected pulses using oscilloscope's cursor to align the vertical cursor with the starting points of each pulse. The rising edges represent the point of maximum signal change and are less affected by noise due to the transition from low to high voltage state (0V to peak), making it the most reliable feature for time measurement.

3.2.2 Exercise 2: Coaxial Cables

The objective of Exercise 2 was to observe the delay time and attenuation factor of pulses sent through coaxial cables of different lengths and terminations. The procedure was as follows:

1. The TEE connector was connected to one output of the waveform generator, with the other end connected to Channel 1 of the oscilloscope and the 15.09 m coaxial cable. The waveform generator was set with a pulse width of 50 ns and a frequency of 15 kHz.
2. The cable was investigated under various load conditions by connecting terminal resistors to the coaxial cable: (a) *Open Circuit (O.C.)* ($Z_L \rightarrow \infty$) with reflection coefficient $r = +1$, where the pulse was reflected in-phase, (b) *Short Circuit (S.C.)* ($Z_L = 0$) with reflection coefficient $r = -1$, where the pulse reflected was inverted (phase shift of π compared to the incident pulse), (c) *Matched Load* ($Z_L = Z_0$) with reflection coefficient $r = 0$, in which no reflection occurs, and (d) *Other Resistive Loads* ($0 < Z_L < \infty$) with partial reflection $-1 < r < +1$.
3. The characteristic impedance Z_0 was found to be 51Ω after connecting terminal resistors to the cable until no reflected pulse was observed.
4. The delay time of the transmitted and reflected pulses was measured to calculate pulse speed and compare it with the theoretical speed based on the cable's dielectric properties, following the methods outlined of task 6 in 3.2.1. The initial and reflected voltages were measured using the oscilloscope to calculate the attenuation factor.

4 Data and Analysis

4.1 Pulses in a Transmission Line

The average time delay values for each LC unit value were plotted in Figure 2. A table containing all recorded values can be found in 6.1. The uncertainty for each data point was determined with:

$$\Delta(\Delta t) = \sqrt{(\Delta t_f)^2 + (\Delta t_i)^2}$$

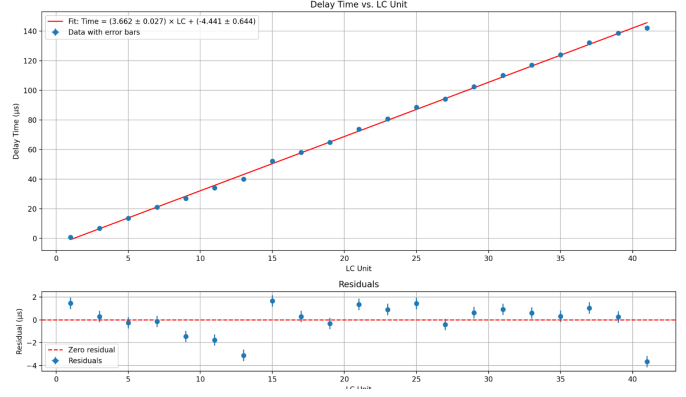


Figure 2: Linear relationship of the average delay time between the transmitted and reflected pulses vs. the number of LC units. Since the LC unit values were discrete numbers, their uncertainty is negligible, so they are not visible.

where Δt_f was the standard deviation of the three trials and Δt_i was the initial time uncertainty. Linear regression analysis in Python yields:

$$t_{\text{delay}} = 3.66 \pm 0.027 \mu\text{s}/\text{LC-unit} \times \text{LC} + (-4.4 \pm 0.64 \mu\text{s})$$

with R-squared (R^2)=0.99, and Reduced Chi-squared (χ^2)=8.69. The R-squared value of 0.99 suggests a high quality of the fit. The reduced Chi-squared of 8.69, which is much higher than the idealized value of 1, suggests that there may still be underestimated systematic errors or uncertainties. The experimental propagation speed of the waves in LC units/s was calculated by inverting the slope of the line:

$$\begin{aligned} v_{\text{experimental}} &= \frac{1}{(3.66170 \times 10^{-6} \pm 0.02657)} \\ &= 0.2731 \times 10^6 \pm 0.0019 \text{ LC-units/s} \end{aligned}$$

The uncertainty in velocity can be found using the formula for the propagation of uncertainty for a reciprocal relationship:

$$\Delta v_{\text{experimental}} = \left| \frac{-1}{m^2} \right| \times \Delta m$$

where m is the slope of the line. The theoretical speed

of propagation can be determined from Equation (1). Instead of considering values per unit length, the component values were used directly to get speed expressed in LC units/s rather than m/s. Given that $C_0 = 0.01 \times 10^{-6}$ F and $L_0 = 1.5 \times 10^{-3}$ H, the speed is calculated as:

$$v_{\text{theoretical}} = \frac{1}{\sqrt{(0.01 \times 10^{-6}) \times (1.5 \times 10^{-3})}} \\ = 0.258 \times 10^6 \text{ LC-units/s}$$

4.2 Pulses in Coaxial Cables

The one-way propagation speed in each cable is deducted to be $v = \frac{2L}{\Delta t}$, where L is the cable length and Δt is the round-trip pulse time. The theoretical delay time was therefore found to be 0.151 μs . Moreover, the speed of light in a vacuum is $c_0 = \frac{1}{\sqrt{\mu_0 \epsilon_0}}$, and in a dielectric medium where $\mu_{\text{actual}} \approx \mu_0$ and $\epsilon_{\text{actual}} = 2.25 \epsilon_0$, the theoretical wave speed becomes:

$$v_{\text{theoretical}} = \frac{1}{\sqrt{\mu_0 (2.25 \epsilon_0)}} \\ = \frac{c_0}{\sqrt{2.25}} \\ \approx 0.67 c_0 = 2.01 \times 10^8 \text{ m/s}$$

Thus signals in the polyethylene-dielectric coaxial cable propagate at about 67% of the theoretical vacuum light speed. Table 1 shows the averaged voltage and time measurements across three trials.

Uncertainties for voltage and time measurements were found using standard error of the mean *sigma \bar{x}* (SEM). The variation in the measurements were reasonably estimated using

$$\sigma = \sqrt{\frac{\sum (x_i - \bar{x})^2}{n - 1}}$$

where x_i is individual measurements, \bar{x} is the mean, and n is the number of measurements. SEM is

(a) Open Circuit and Short Circuit

	O.C.	S.C.
V_i (V)	1.280 ± 0.0029	5.150 ± 0.0043
V_f (V)	-0.125 ± 0.0030	-4.010 ± 0.0061
t_i (μs)	599.99 ± 0.078	599.78 ± 0.049
t_f (μs)	600.143 ± 0.0040	599.93 ± 0.016
Δt (μs)	0.16 ± 0.078	0.16 ± 0.051
v (m/s)	$1.95 \times 10^8 \pm 6.6 \times 10^6$	$1.92 \times 10^8 \pm 2.0 \times 10^7$

(b) Resistive Loads (51 Ω and 100 Ω)

	M.I. (51 Ω)	100 Ω
V_i (V)	3.15 ± 0.010	2.650 ± 0.0036
V_f (V)	N/A	-1.375 ± 0.0047
t_i (μs)	599.92 ± 0.035	599.99 ± 0.012
t_f (μs)	N/A	600.15 ± 0.051
Δt (μs)	N/A	0.15 ± 0.052
v (m/s)	N/A	$1.96 \times 10^8 \pm 6.5 \times 10^7$

Table 1: Measurements for Cable 1 (15.09 m \pm 0.02 m). T_{initial} measures the moment the incident pulse is generated, while T_{final} records when the reflected pulse returns to Channel 1. It's found that the characteristic impedance Z_0 of the coaxial cable is 51 Ω since no reflection was detected.

found to be $\sigma_{\bar{x}} = \frac{\sigma}{\sqrt{n}}$. It's found through uncertainty propagation that uncertainty in delay time is $\Delta(\Delta t) = \sqrt{(\Delta t_f)^2 + (\Delta t_i)^2}$, and uncertainty in experimental velocity is:

$$\Delta v_{\text{experimental}} = v_{\text{experimental}} \times \sqrt{\left(\frac{\Delta L}{L}\right)^2 + \left(\frac{\Delta(\Delta t)}{\Delta t}\right)^2}$$

Additionally, the attenuation of the cable was evaluated using Equation 4. The attenuation factors were determined based on the voltage measurements provided in Table 1.

The uncertainty of the attenuation factor is found to be $\Delta A = \frac{20}{\ln(10)} \sqrt{\left(\frac{\Delta V_{\text{reflected}}}{V_{\text{reflected}}}\right)^2 + \left(\frac{\Delta V_{\text{initial}}}{V_{\text{initial}}}\right)^2}$. The uncertainty in attenuation per meter is $\frac{\Delta A}{L} = \frac{A}{L} \sqrt{\left(\frac{\Delta A}{A}\right)^2 + \left(\frac{\Delta L}{L}\right)^2}$.

Termination	Attenuation (dB/m)
Open Circuit	-1.34 ± 0.012
Matched Impedance ($51\ \Omega$)	N/A
Short Circuit ($Z_L = 0$)	-0.1440 ± 0.00081
$100\ \Omega$	-0.378 ± 0.0016

Table 2: Attenuation Measurements for Cable 1 ($15.09\text{ m} \pm 0.02\text{ m}$). The negative sign in the attenuation factor means indicates loss in signal and energy during transmission.

5 Discussion and Conclusion

5.1 Pulses in Transmission Line

5.1.1 Delay Time

To minimize human eye-balling error in determining the starting point of each waveform, several techniques were implemented. A threshold x-value was set at the point where the pulses began, and the y-value cursor was aligned to this threshold for both waveforms. Since the transmitted pulse has a square wave pulse, its starting point was easily identified by zooming in on the rising edge. For the reflected pulse, which had a curved incline with small sinusoids, the cursor was placed at the point where the initial increase in waveform was observed (Figure 5). This procedure was repeated three times for each data point to take the average. The uncertainty in delay time was determined using the standard deviation of the measured delay times and propagated accordingly.

5.1.2 Error Analysis

The experimental wave propagation speed was determined from the slope of the delay time vs. number of LC units graph, yielding a value of $v_{\text{experimental}} = 2.73 \times 10^5$ LC-units/s. The theoretical speed, calculated using the given component values, was $v_{\text{theoretical}} = 2.582 \times 10^5$ LC-units/s. The 5.81% discrepancy between the experimental and theoretical speeds suggests a relatively close alignment but still

indicates the presence of non-idealized components in the experimental setup. Several sources of error could contribute to the observed discrepancy:

- The negative intercept ($-4.44097 \pm 0.64402\ \mu\text{s}$) suggests a delay in the circuit, possibly due to the response delay or resistance to contact on the internal wire. The delay time should ideally be zero when $N = 0$ (no LC units). The uncertainty of ± 0.64402 is small compared to the magnitude of the intercept, suggesting that the intercept is not significant.
- A reduced chi-squared value of 1 is ideal for a good fit to the data, but $\chi_n^2 = 8.695$ is much greater than 1.
- Real inductors and capacitors exhibit resistive losses, mutual inductance, and stray capacitance that could deviate from ideal characteristics of wave propagation.

For future improvements, several modifications can be made: using higher precision components with tighter tolerance ratings (e.g., capacitors and inductors with $\pm 1\%$ instead of $\pm 5\%$ variability), using an oscilloscope with higher sampling rate, or optimizing circuit layout by shielding wires to reduce unwanted electromagnetic coupling.

5.2 Pulses in Coaxial Cable

5.2.1 Delay Time

It was hypothesized that the wave propagation speed remains largely unchanged regardless of whether the cable is open, short-circuited, or terminated with a resistive load, while the reflections and standing wave patterns vary. This hypothesis was confirmed in Exercise 2, where the theoretical delay time of $0.151\ \mu\text{s}$, calculated using the speed of light adjusted for the dielectric properties of the coaxial cable, falls within the uncertainty range of all measured cases. The percentage errors were determined to be 5.62% for the

open circuit, 5.62% for the short circuit, and 0.6% for the termination of $100\ \Omega$, all of which indicate a high degree of precision.

The results align with expectations, as only the dielectric material of the coaxial cable significantly influences the signal propagation speed. The slight variations in experimental delay time likely stem from experimental uncertainties, such as difficulty in precisely identifying the signal arrival time on the oscilloscope, even when averaging multiple trials. Additionally, small variations in cable properties, instrument calibration tolerances, and signal dispersion effects may contribute to the minor discrepancies observed. Future improvements could involve using higher-resolution measurement tools and minimizing external noise sources to enhance precision.

5.2.2 Attenuation

For the pulse evaluation in coaxial cables, the oscilloscope's effect on reflections can be safely ignored. The large input impedance of the oscilloscope, much greater than the characteristic impedance of the coaxial cable ($51\ \Omega$), allows only a negligible amount of current to flow into it, leaving the signal behavior and reflections unaffected.

From Table 2 it was observed that the open circuit exhibited the highest attenuation (-1.34 ± 0.012 dB/m), while the short circuit showed the least attenuation (-0.378 ± 0.0016 dB/m). Other resistive terminations resulted in intermediate attenuation values. These findings align with theoretical expectations. In an open circuit, the extremely high load impedance causes significant electric field buildup at the termination, leading to energy loss primarily as dielectric heating in the cable insulation[2]. Despite the theoretical reflection coefficient being $r \approx +1$, the open circuit results in the most energy dissipation.

In contrast, a short circuit has a low-impedance termination that allows current to flow directly, with magnetic field energy dominating at the termination point. Ideally, the incident and reflected voltages in a short circuit should have the same magnitude but opposite polarity. However, the experimental reflected voltage $V_f = -4.010 \pm 0.0061V$ is lower than the theoretical value $V_{f\text{ theoretical}} = -5.150 \pm 0.0043V$, indicating resistive losses in the cable and conductors. These losses are generally smaller than the dielectric losses in an open circuit, where the experimental reflected voltage $V_f = -0.125 \pm 0.0030V$ deviates significantly from the theoretical value $V_{f\text{ theoretical}} = 1.280 \pm 0.0029V$. Additional factors contributing to energy dissipation may include cable imperfections such as manufacturing tolerances, material non-uniformities, and disturbances in instrument calibration.

6 Bibliography

- [1] PHY294. Pulses in Cables. Year Accessed (2025).
- [2] N. B. Kardile, A. Sinha, and others, "Electric and magnetic field-based processing technologies for food," in *Current Developments in Biotechnology and Bioengineering*, 2022. Available: <https://sciencedirect.com/topics/chemical-engineering/dielectric-heating>

Appendix

6.1 Datasets for pulses in Transmission Line

LC Unit	Trial 1 (us)	Trial 2 (us)	Trial 3 (us)	Average (us)
1	0.67	0.69	0.68	0.68
3	6.83	6.85	6.85	6.84
5	13.61	13.63	13.61	13.62
7	21.05	19.04	20.1	20.06
9	27.07	26.21	27.02	26.77
11	34.07	34.05	33.98	34.03
13	40.05	42.51	41.2	41.25
15	52.15	52.11	48.41	50.89
17	58.09	58.2	58.6	58.30
19	64.81	68.75	65.3	66.29
21	73.81	71.2	72.51	72.51
23	80.68	81.4	81.29	81.12
25	88.54	87.34	86.3	87.39
27	94.01	94.51	95.06	94.53
29	102.38	102.95	103.2	102.84
31	109.99	109.29	108.2	109.16
33	116.99	117.3	116.95	117.08
35	124.03	125.45	124.6	124.69
37	132.08	132.4	134.05	132.84
39	138.62	139.45	138.06	138.71
41	142.02	142.67	145.38	143.36

Figure 3: Screenshot of raw data across three trials and average time delay

6.2 Code for Exercise 1

https://drive.google.com/file/d/1pvwiaTNmrp_Knd0G5kqVV0IZdvu7QPXo/view?usp=drive_link

6.3 Experimental Methodology



Figure 4: Photos of experimental setup

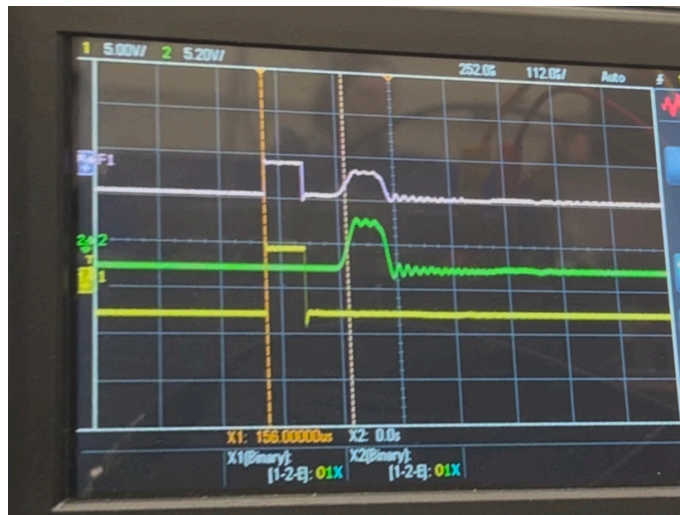


Figure 5: Photo of oscilloscope displaying the waveforms of the transmitted and reflected pulses

6.4 Various Cases Evaluated in Coaxial Cable

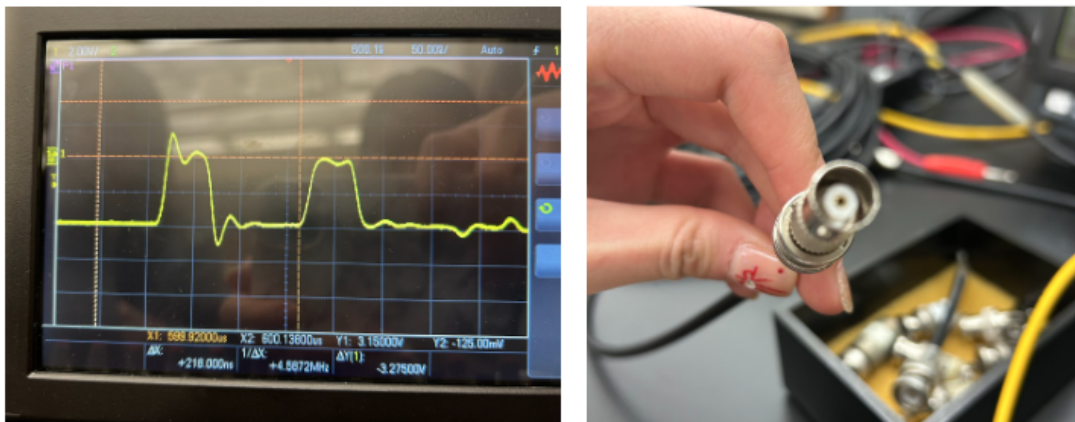


Figure 6: Open circuit



Figure 7: Short circuit

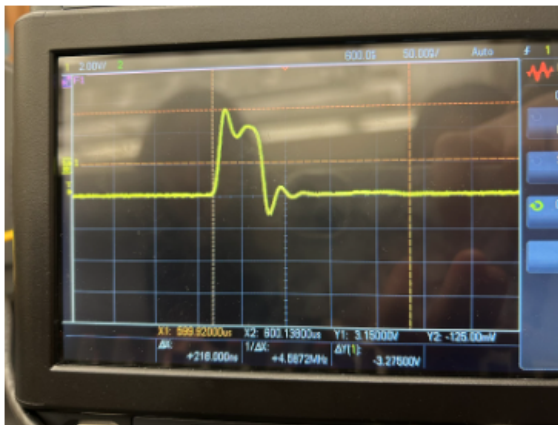


Figure 8: 51 Ω

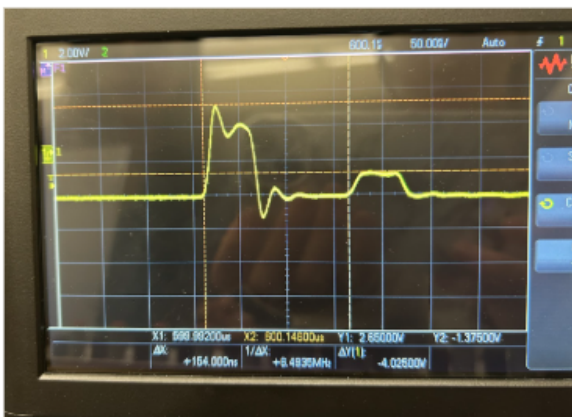


Figure 9: 100 Ω